Journal of the European Ceramic Society 19 (1999) 1873–1881

PII: S0955-2219(98)00290-8
0955-2219/99/$ - see front matter

Relationships between Sintering Conditions, Microstructure and Dielectric Properties of Lead Iron Niobate

Supon Ananta and Noel W. Thomas*

Department of Materials, University of Leeds, Leeds LS2 9JT, UK

(Received 1 September 1998; accepted 28 November 1998)

Abstract

Lead iron niobate, $Pb(Fe_{1/2}Nb_{1/2})O_3$ (PFN) ceramics have been produced by sintering PFN powders synthesized from lead oxide (PbO) and iron niobate ($FeNbO_4$), with an effective method developed for minimising the level of PbO loss during sintering. Attention has been focused on relationships between sintering conditions, phase formation, density, microstructural development and dielectric properties. The sintering temperature has been found to have a pronounced effect on the density, grain growth and dielectric properties of the sintered PFN ceramics, with maximum density and relative permittivity values obtained under sintering conditions of 1175°C for 2 h. The origin of the strong dependence of values of ε_r and tan δ on frequency is discussed. © *1999 Elsevier Science Limited. All rights reserved*

Keywords: lead iron niobate PFN, sintering, microstructure: final, dielectric properties.

1 Introduction

Lead iron niobate ($Pb(Fe_{1/2}Nb_{1/2})O_3$; PFN) is one of the family of lead-based complex perovskites which is of interest as a component in commercial electroceramic materials. Moreover, it is typically characterised by high relative permittivities and low sintering temperatures. Work by Lejeune and Boilot[1] has indicated that PFN is formed indirectly via a sequence of intermediates, some of these being lead niobium oxide pyrochlores. It was also proposed that formation of a perovskite PFN phase requires a high reactivity of ferric oxide, Fe_2O_3, with other phases in the PbO-Nb_2O_5 system.

A technological problem in working with PFN is the need to control its dielectric loss: although acceptable levels for tan δ would be 0·01–0·03, depending on the application,[2] further reductions are clearly desirable. Owing to the dependence of dielectric loss on many variables, i.e. chemical composition, microstructure, processing history, trace impurities, temperature and measuring frequency, a systematic study of the phenomenon would be non-straightforward. An alternative approach, which is followed here, is to pay close attention to critical processing variables, and to monitor the effects on dielectric loss.

In this work, consideration is given to the synthesis, fabrication and characterisation of PFN prepared by a modified two-stage mixed oxide route. The study encompasses identification of phases, elemental distributions, pyrochlore formation, microstructure and dielectric response. As there are only a few articles devoted to PFN itself, whether in single crystal[3–5] or ceramic form,[6–8] this article should be seen as a contribution towards developing a more complete knowledge of the properties of this material.

2 Method

Lead iron niobate (PFN) powder was synthesised from commercially available oxides using a modified mixed oxide synthetic route described in earlier work.[9] In this method, $FeNbO_4$ precursors were prepared from the reaction between Fe_2O_3 (>99%, Alfa) and Nb_2O_5 (>99·9%, Alfa) at 1150°C for 4 h, prior to reaction with PbO (>99·9%, Aldrich) at 800°C for 3 h to form the final product of PFN powder. Ceramic fabrication

*To whom correspondence should be addressed at present address: WBB Technology Ltd., Watts Blake Bearne & Co plc, Park House, Courtenay Park, Newton Abbot TQ12 4PS, UK. Fax: +44 (0)1626 322386; e-mail: nthomas@wbb.co.uk

was achieved by adding 3 wt% polyvinyl alcohol (PVA) binder, prior to pressing as pellets in a pseudo-uniaxial die press at 100 MPa. Using an arrangement of green pellets previously reported in our PMN study,[10] four sets of sintering experiments were carried out (Fig. 1): (i) in air, (ii) inside a closed alumina crucible, (iii) inside a closed alumina crucible containing a PFN atmosphere powder; and (iv) inside a platinum foil and closed alumina crucible with PFN atmosphere powder. Green pellets were placed between PFN setters, with the binder burnt out at 500°C for 4 h. The PFN pellets were extracted for weighing, to verify that all the binder had been removed. The dimensions of the green pellets were also measured and the surfaces of the setter pellets repolished before reinserting into the alumina crucible, together with PFN atmosphere powder. Sintering was carried out at 1075 to 1175°C for 2 h, with constant heating rates of 10°C min^{-1} applied. Densities of the sintered pellets were determined by using the Archimedes principle. XRD was used to examine the phases formed, with the microstructural development examined by scanning electron microscopy (SEM). The dielectric properties of the final products were measured at various frequencies between 100 and 100 kHz in the temperature range from −60 to 180°C, using an HP4284A precision LCR meter in conjunction with a Delta Design 9023 temperature chamber.

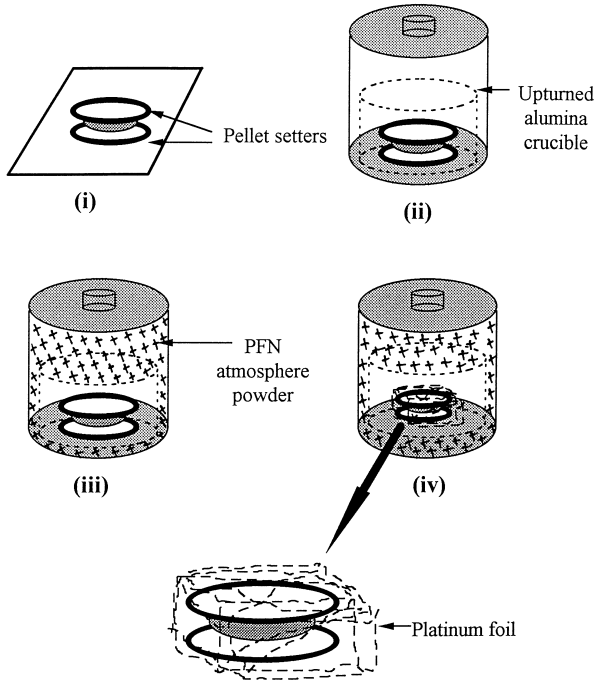

Fig. 1. Schematic representations of the experimental set-up for four sintering conditions: (i) in air; (ii) inside a closed alumina crucible, (iii) inside a closed alumina crucible containing a PFN atmosphere powder; and (iv) inside a platinum foil and closed alumina crucible with atmosphere powder.

3 Results and Discussion

3.1 Densification analysis

The degree of PbO volatilisation during the sintering of PFN may be calculated for each sample by recording the weights of the pellets before and after sintering. Weight loss data of all samples sintered at 1075 to 1175°C for 2 h are shown in Fig. 2. Whereas, in general, the weight loss increases with sintering temperature, it is interesting to note that the level of lead loss can be effectively minimised by employing platinum foil and PFN atmosphere powder, as in the methodology adopted for the earlier PMN study.[10] A density of about 90–96% of the maximum value for PFN could be achieved in this way (Table 1; Fig. 3). The maximum density was obtained by sintering method (iv) at 1175°C. Critical damage, with some melted areas has been observed in PFN ceramics sintered at 1200°C.

3.2 Analysis of phases formed

XRD patterns of the PFN ceramics formed at various sintering temperatures are given in Fig. 4. The strongest reflections in the majority of all XRD traces indicate formation of the PFN perovskite phase, which could be matched with JCPDS file 32-522. To a first approximation, this major phase has a cubic perovskite-type structure in space group *Pm3m* (No. 221), with cell parameter $a = 401$ pm. The tetragonal pyrochlore-type structure of $Pb_2Fe_2O_5$ (JCPDS file 34-871) with cell parameters $a = 779$ pm and $c = 1578$ pm was found as the only minor phase alongside the majority perovskite PFN phase.

The relative amounts of perovskite and pyrochlore phases present in each sintered ceramic were calculated from the intensities of the major X-ray reflections from the respective phases. In this connection, the following approximation was adopted, as in the earlier PMN study:[10]

$$\text{wt\% perovskite phase} = \left(\frac{I_{\text{Perov}}}{I_{\text{Perov}} + I_{\text{Pyro}}}\right) \times 100 \quad (1)$$

Here I_{Perov} and I_{Pyro} refer to the intensities of the {110} perovskite and {220} pyrochlore peaks, respectively, these being the most intense reflections in the XRD patterns of both phases. For the purposes of estimating the concentrations of pyrochlore phase present, eqn (1) has been applied to the diffraction patterns obtained (Table 1).

The effect of sintering temperature (in the range from 1075 to 1175°C) on phase formation was found to be insignificant. Only small amounts of

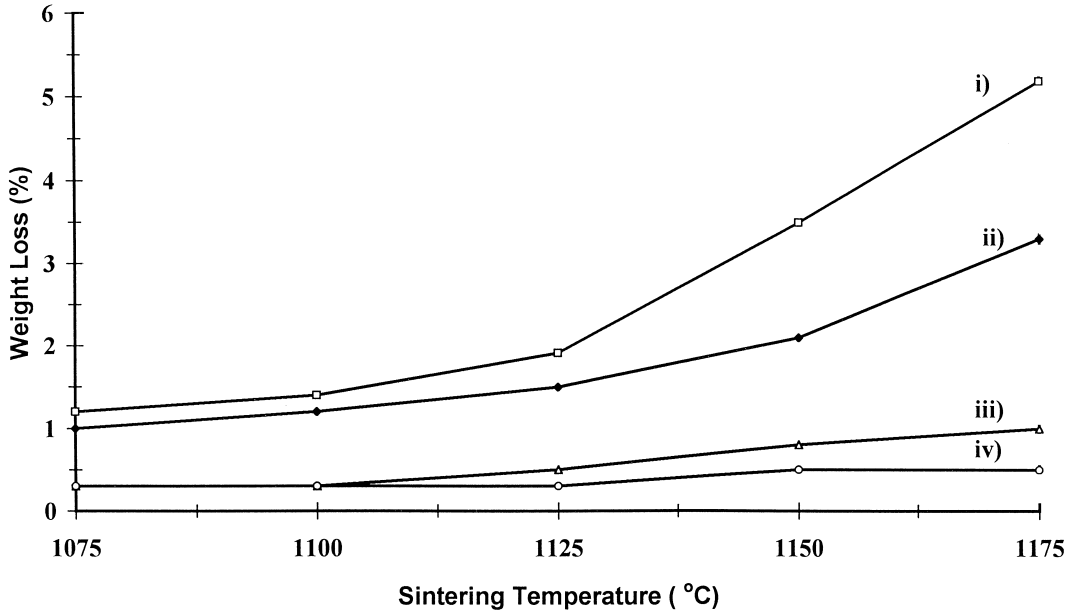

Fig. 2. Weight loss as a function of the sintering temperature in PFN ceramics sintered: (i) in air; (ii) inside a closed alumina crucible, (iii) inside a closed alumina crucible containing a PFN atmosphere powder; and (iv) inside a platinum foil and closed alumina crucible with atmosphere powder.

Table 1. Effect of sintering temperature on phase formation and densification in sintered PFN ceramics

Sintering temperature (°C)/2 h	Perovskite *(wt%)*	*Pyrochlore (wt%)*	*Density* (%)*
1075	99·5	0·5	90
1100	100·0	0·0	92
1125	100·0	0·0	94
1150	100·0	0·0	95
1175	100·0	0·0	96

*Theoretical density value of PFN is $\sim$8·457 g cm^{-3}. The data were taken from samples sintered under condition (iv). The estimated precision of the concentration value for the two phases is $\pm$0·1%.

pyrochlore $Pb_2Fe_2O_5$ were detected in samples sintered at 1075°C for 2 h. A single phase of perovskite PFN (yield of 100% within the limitations of the XRD technique) was obtained in samples sintered at 1100 to 1175°C. This is probably due to the effectiveness of vibro-milling and a carefully optimised reaction to form single-phase precursor powders. Moreover, the degree of lead loss during sintering is probably below the level which normally leads to pyrochlore formation.

3.3 Microstructural analysis

Microstructural development during sintering was investigated by scanning electron microscopy (SEM). Micrographs of free and fracture surfaces of PFN ceramics sintered at various temperatures from 1075 to 1175°C are shown in Fig. 5. The results indicate that grain size tends to increase with sintering temperature, as in the PMN study.[10] The microstructure becomes denser as the sintering temperature increases, as indicated by the grain packing and increases in grain boundary thickness.

3.4 Dielectric response of the ceramics

The variation of relative permittivity and dissipation factor with temperature for the five sets of sintering conditions is shown in Fig. 6. As the sintering temperature is increased to 1175°C, both relative permittivity, ε_r and dissipation factor, tan δ increase for a given frequency, as shown for the 1 kHz data in Fig. 7. The systematic increase in maximum relative permittivity with sintering temperature is likely to be due to increased conductivity in the samples, in accordance with a mechanism proposed below. The temperatures of maximum relative permittivity and maximum dissipation factor are summarised in Tables 2 and 3. A straightforward assessment of the level of frequency dispersion is provided by the parameter $\Delta T = T(\varepsilon_{r,\max})_{100\,\mathrm{kHz}} - T(\varepsilon_{r,\max})_{100\,\mathrm{Hz}}$, as previously employed[10]. The variation of maximum relative permittivity and dissipation factor with sintering temperature is given in Figs 8 and 9, for all frequencies.

There are two possible mechanisms of electronic conductivity at higher temperatures which are worthy of consideration. First, it is possible that there is some residual $FeNbO_4$ in the sintered ceramic, this having been used as a reaction intermediate to the PFN powders.[11] Since this compound is known to show semiconductive properties,[12] it could be responsible for the high values of ε_r and tan δ which are observed in this work, but have not been revealed in previous studies, some of which have been concerned with single crystals. In this

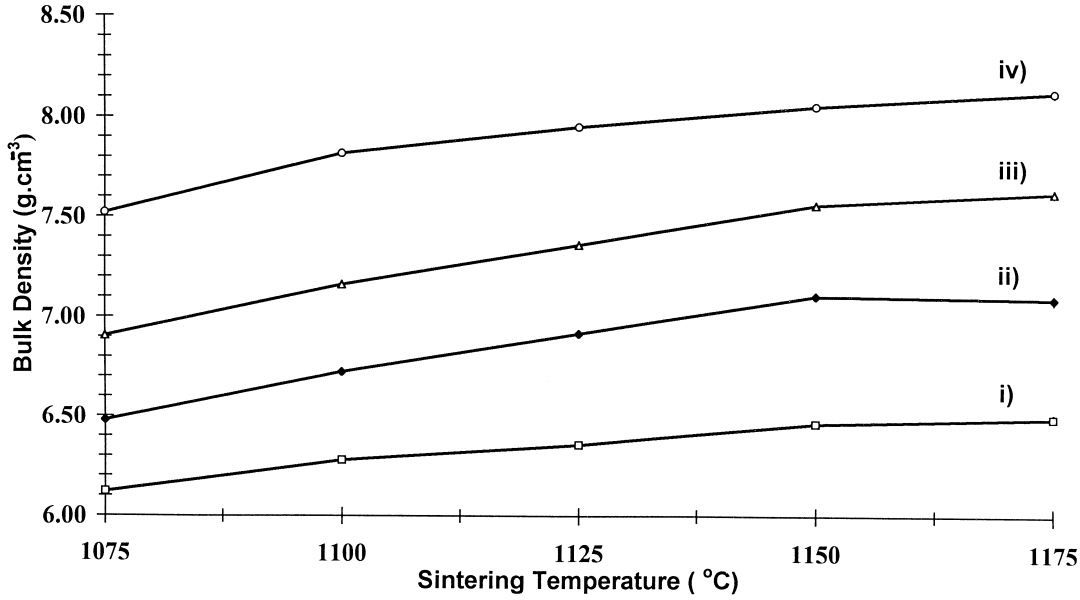

Fig. 3. Dependence of bulk density on the sintering temperature in PFN ceramics sintered: (i) in air; (ii) inside a closed alumina crucible, (iii) inside a closed alumina crucible containing a PFN atmosphere powder; and (iv) inside a platinum foil and closed alumina crucible with atmosphere powder.

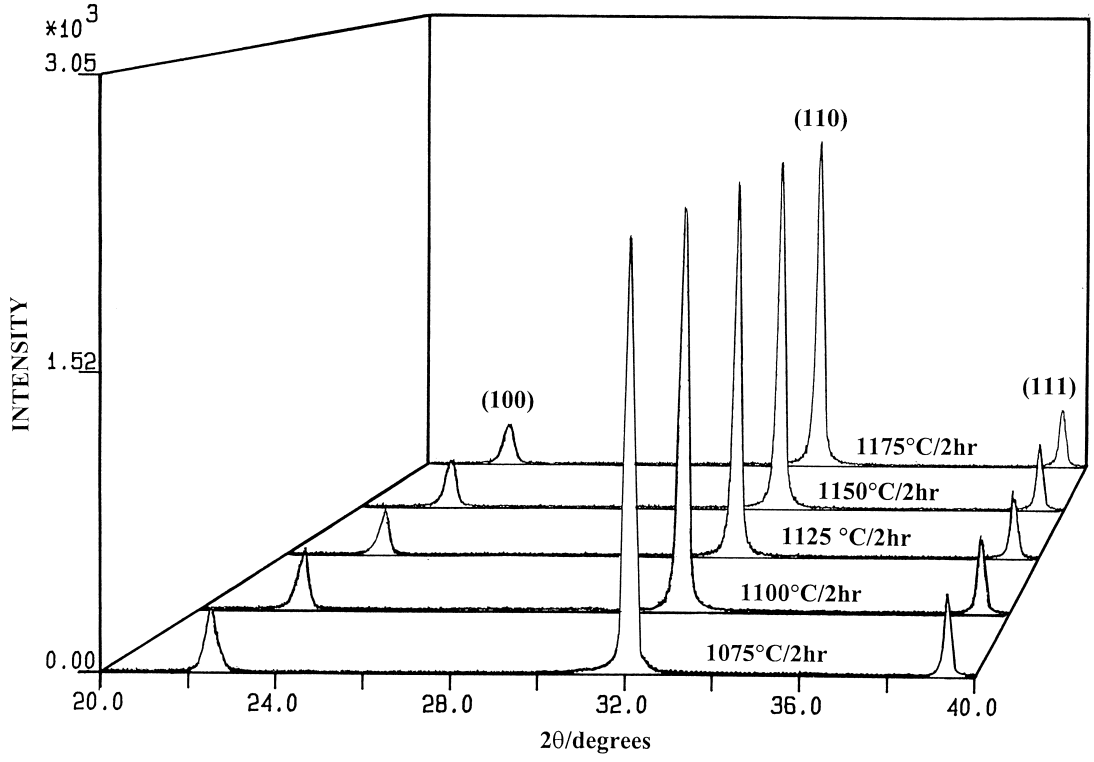

Fig. 4. XRD patterns of PFN ceramics sintered at various sintering temperatures.

connection, some model studies of two-phase PFN–$PbFeNbO_4$ systems would reveal the nature and extent of this possible problem.

Another possibility, which in our view should also be investigated further, is that the concentration of Fe^{2+} ions in the sintered PFN ceramics could be highly sensitive to sintering temperature. As is widely known, the co-existence of Fe^{2+} and Fe^{3+} ions on equivalent crystallographic sites can frequently give rise to an electron-hopping type of conduction mechanism, which, owing to finite hopping (or jump) probabilities, tends to come into effect at lower frequencies. This mechanism would be consistent with the strong dependence of relative permittivity and dissipation factor on frequency, which is observed in Figs 6 and 7.

A possible reaction for the formation of Fe^{2+} ions, formally represented by $[Fe'_{Fe}]$ in Kröger-Vink notation, would be:

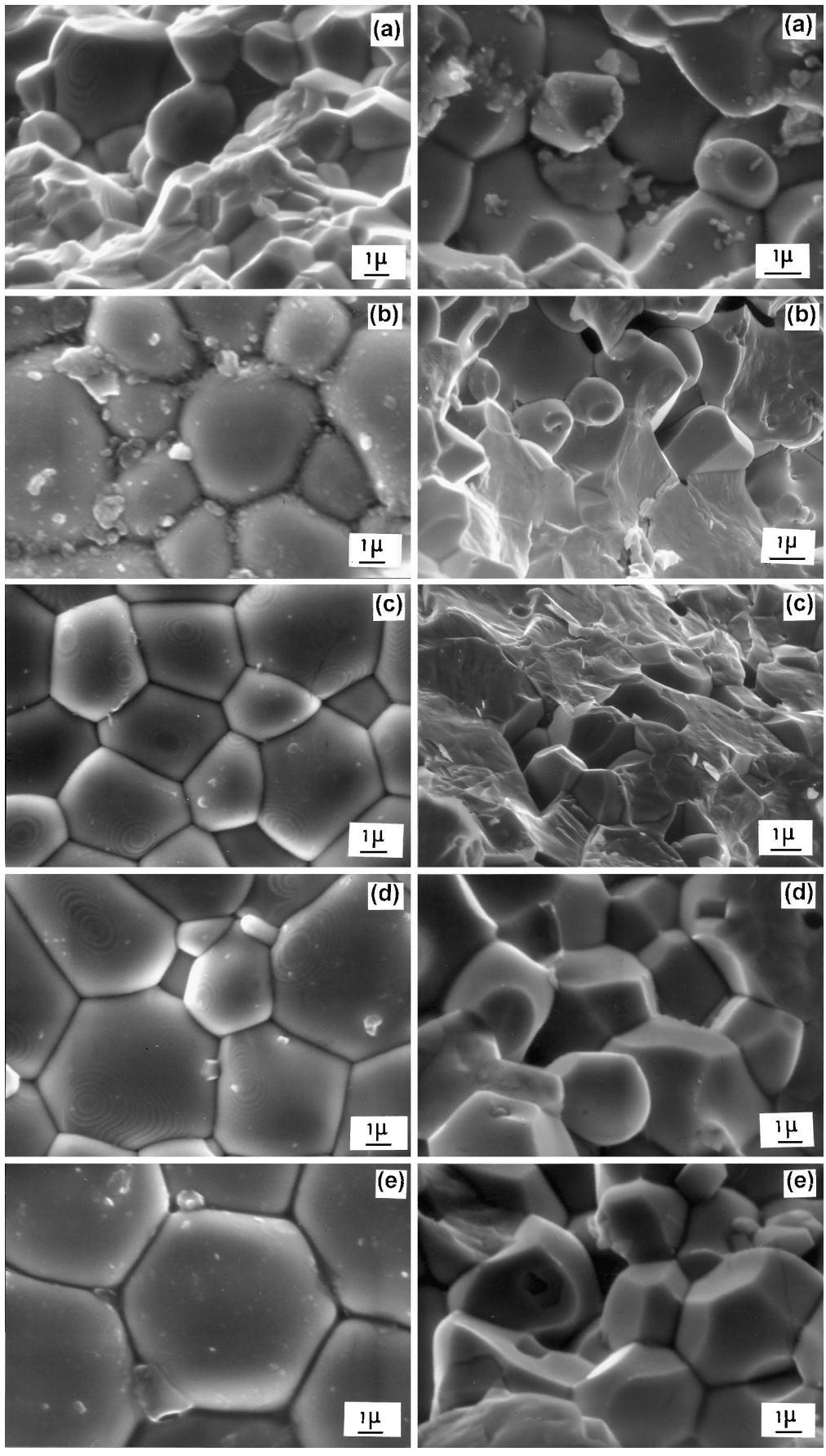

Fig. 5. SEM micrographs of free and fracture surfaces of PFN ceramics sintered at (a) 1075°C, (b) 1100°C, (c) 1125°C, (d) 1150°C and (e) 1175°C.

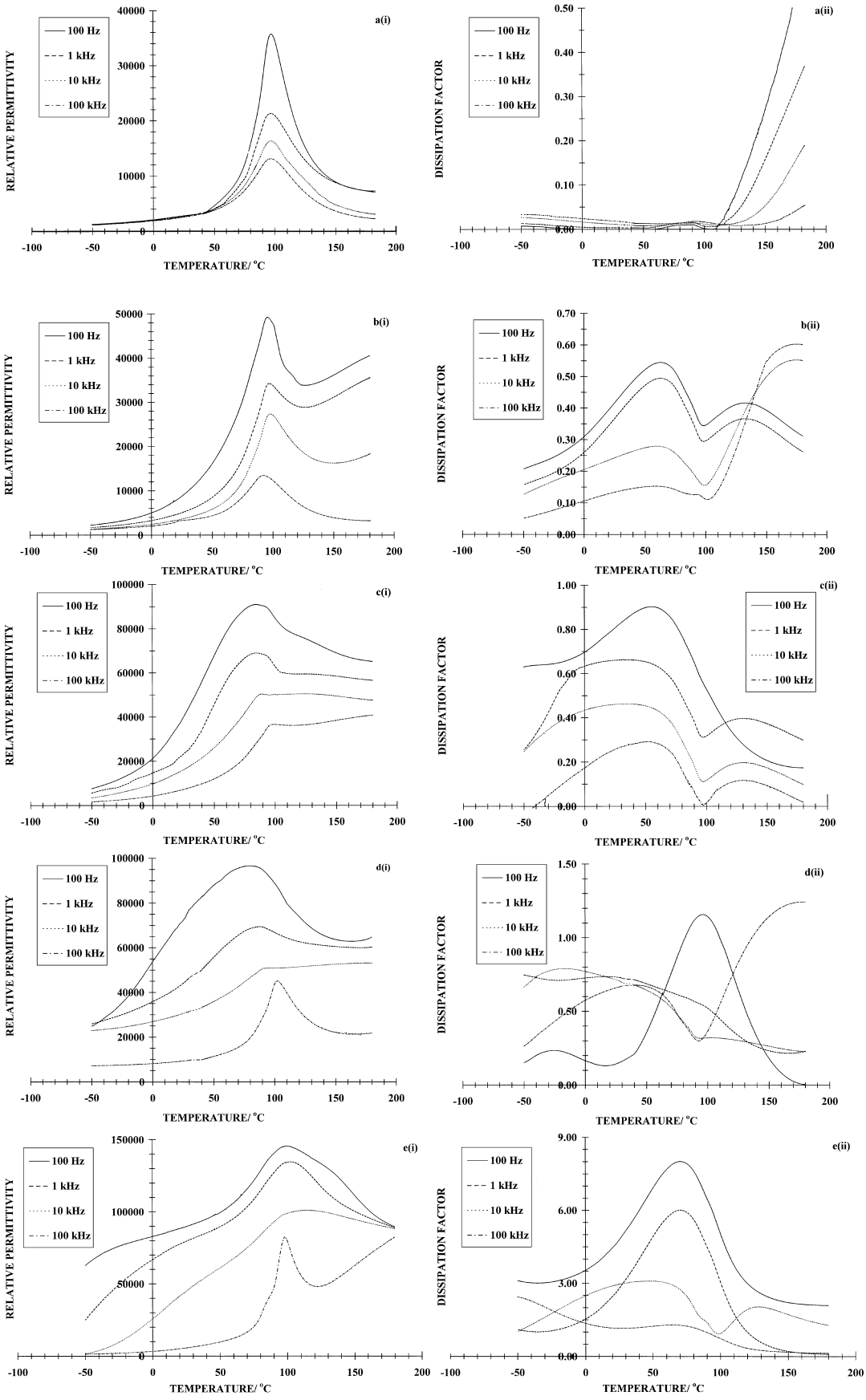

Fig. 6. Variation of (i) relative permittivity and (ii) tan δ for PFN ceramics sintered at (a) 1075°C, (b) 1100°C, (c) 1125°C, (d) 1150°C and (e) 1175°C.

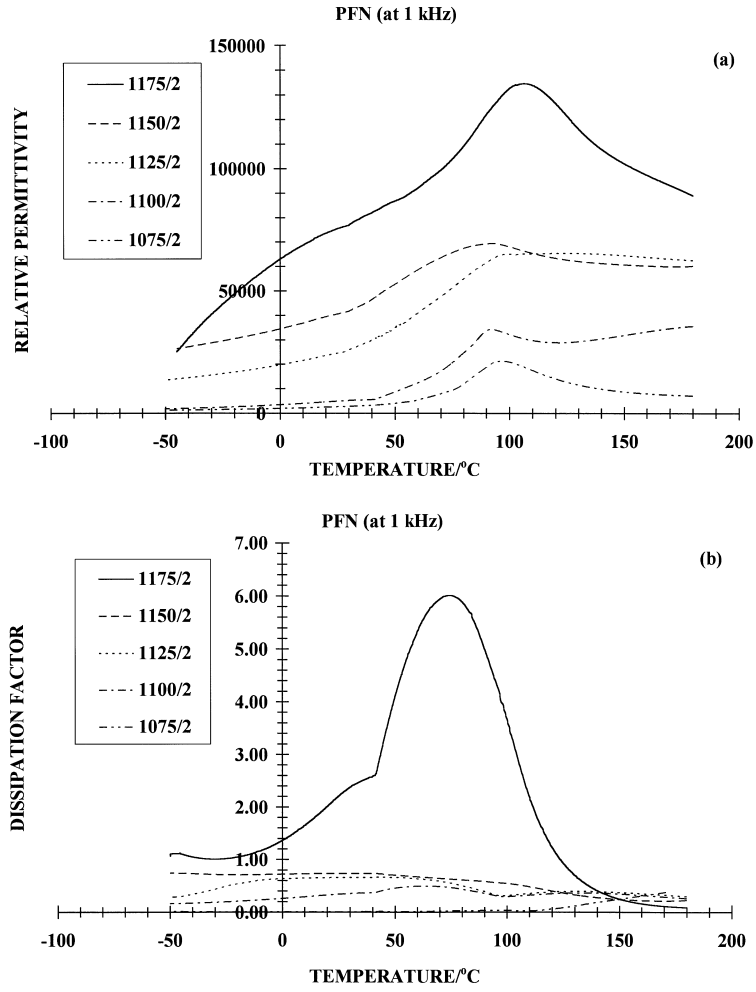

Fig. 7. Comparison of dielectric response at 1 kHz for different sintering temperatures; (a) Relative permittivity (b) Dissipation factor.

Table 2. Variation in temperatures of maximum relative permittivity $T(\varepsilon_{r,\max})$ with the sintering temperature and frequency measurements

Sintering temperature (°C)	$T(\varepsilon_{r,max})$				ΔT
	100 Hz	*1 kHz*	*10 kHz*	*100 kHz*	
1075	106·5–107·6	105·7–108·1	105·7–108·1	105·4–108·1	1–2
1100	105·5–106·6	106·9–107·7	107·7–108·5	101·1–113·6	4–7
1125	93·9–96·1	93·9–96·1	99·0–99·6	108·4–110·0	14
1150	87·0–92·3	97·3–98·8	101·3–101·6	112·1–112·7	20–24
1175	109·1–109·9	111·3–113·7	117·0–132·7	108·0	1–2

Table 3. Variation in temperatures of maximum dissipation factor $T(\varepsilon''_{r,max})$ with sintering temperature and frequency measurements

Sintering temperature (°C)	$T(\varepsilon''_{r,max})$				ΔT
	100 Hz	*1 kHz*	*10 kHz*	*100 kHz*	
1075	80·2–80·5	64·1–61·2	56·1–62·8	52·2–63·9	9
1100	61·2–64·1	64·1–61·2	56·1–62·8	52·2–63·9	9
1125	53·1–57·9	34·9–37·4	34·9–37·4	51·1–53·4	2–5
1150	94·3–98·1	15·5–19·0	101·0–105·9	40·2–43·8	54–55
1175	68·9–71·5	69·0–71·5	45·2–50·6	60·7–67·9	4–8

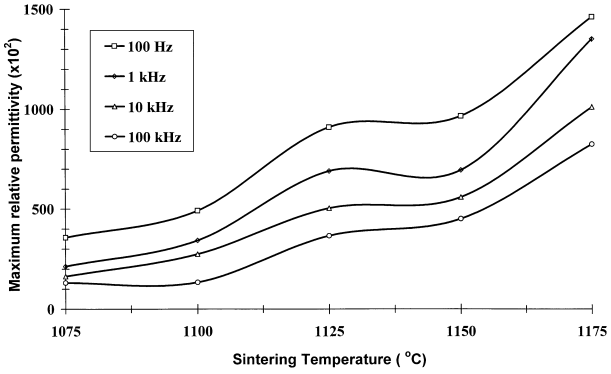

Fig. 8. Variation of the maximum relative permittivity of PFN ceramics with sintering temperature.

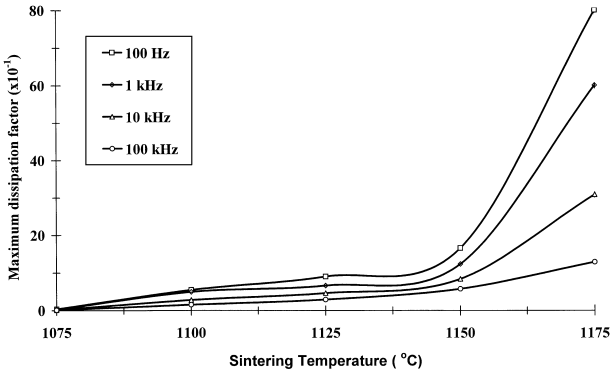

Fig. 9. Variation of the maximum dissipation factor of PFN ceramics with sintering temperature.

$$O_o \Longleftrightarrow V_o^{\cdot\cdot} + 2Fe'_{Fe} + \frac{1}{2}O_2(g), \qquad (2)$$

from which, according to the law of Mass Action,

$$[Fe'_{Fe}] = \left(\frac{K}{[V_{\ddot{O}}]}\right)^{\frac{1}{2}} P_{O_2}^{-\frac{1}{4}}, \qquad (3)$$

where K is the equilibrium constant.

Whereas the experimental work carried out here suggests that this reaction is suppressed at lower sintering temperatures, eqn (3) implies that there are two further means of reducing $[F'_{e_{Fe}}]$. The first technique would be to sinter in oxygen, thereby increasing P_{O_2}. Alternatively, $[V_o^{\cdot\cdot}]$ could be increased by chemical doping. A method of doing this would be to engineer a degree of non-stoichiometry in the PFN product, such as a composition

$$Pb_2(Fe^{3+}_{1+\delta}Nb^{5+}_{1-\delta})O_{6-\delta}$$

whereby oxygen vacancies are introduced extrinsically. Morever, subsequent work by Chiu and Desu[13] has indicated that the d.c. conductivity and the dissipation factor of PFN, which were attributed to electron hopping by the formation of $[Fe'_{Fe}]$, can be reduced by the addition of Li_2CO_3. These considerations should form part of a future study of the sintering behaviour of PFN.

In addition, there are other significant factors such as impurities, heating rates, sintering times and microstructural features, i.e. grain size distribution, grain boundary structure and pyrochlore distribution, which share responsibility in determining the dielectric response of the final sintered products. Although pyrochlore content, lead volatilisation and low densification correlate with a deterioration in the maximum value in relative permittivity, no simple, unifying mechanism has been proposed to date.

The ultimate choice of sintering temperature will depend on an assessment of the material requirements. For example, the use of cheaper metal electrodes would dictate the use of lower sintering temperatures, despite the smaller expected values of permittivity and density, the latter capable of being increased by hot isostatic pressing. By comparison, any gains in density and permittivity from samples sintered at higher sintering temperatures would be associated with higher values of dielectric loss, this being generally regarded as disadvantageous in the majority of electronic applications.

4 Conclusion

PFN ceramics of high density and optimised dielectric properties may be produced by employing a straightforward sintering procedure at temperatures between 1075 and 1175°C for 2 h. Also required are the use of pyrochlore-free PFN starting powders (derived from industrial grade precursors) and a sintering method employing platinum foil and a PFN atmosphere powder.

Acknowledgements

The authors wish to thank Dr. D. A. Hall (Manchester Materials Science Centre) for his kindness in confirming the results obtained for the dielectric properties of PFN. Thanks also are due to Dr. D. Hind for experimental assistance and helpful discussions. One of the authors (SA) wishes to express his gratitude to the DPST project and to the Thai Government for financial support.

References

1. Lejeune, M. and Boilot, J. P., Formation mechanism and ceramic process of the ferroelectric perovskites: Pb$(Mg_{1/3}Nb_{2/3})O_3$ and Pb$(Fe_{1/2}Nb_{1/2})O_3$. *Ceram. Inter.*, 1982, **8**, 99–103.
2. Kassarjian, M. P., A lead–iron–niobate dielectric ceramic for low firing temperature capacitors. M.S. thesis, Pennsylvania State University, University Park, PA, 1984.

3. Brunskill, I.H., Schmid, H. and Tissot, P., The characterization of high temperature solution-grown single crystals of $Pb(Fe_{1/2}Nb_{1/2})O_3$. *Ferroelectrics*, 1981, **37**, 547–550.
4. Bokov, A. A. and Emelyanov, S. M., Electrical properties of $Pb(Fe_{0\cdot5}Nb_{0\cdot5})O_3$ crystals. *Phys. Stat. Sol.(b)*, 1991, **164**, K109–K112.
5. Bonny, V., Bonin, M., Sciau, P., Schenk, K. J. and Chapuis, G., Phase transitions in disordered lead iron niobate: X-ray and synchrotron radiation diffraction experiments. *Solid State Comm.*, 1997, **102**, 347–352.
6. Yasuda, N. and Ueda, Y., Dielectric properties of $PbFe_{1/2}Nb_{1/2}O_3$ under pressure. *Ferroelectrics*, 1989, **95**, 147–151.
7. Yokosuka, M., Electrical and electromechanical properties of hot-pressed $Pb(Fe_{1/2}Nb_{1/2})O_3$ ferroelectric ceramics. *Jpn. J. Appl. Phys.*, 1993, **32**, Part 1– 3A 1142–1146.
8. Fu, S. L. and Chen, C. F., Fabrication of perovskite $Pb(Fe_{1/2}Nb_{1/2})O_3$ and reaction mechanism. *Ferroelectrics*, 1989, **82**, 119–126.
9. Ananta, S. and Thomas, N. W., A modified two-stage mixed oxide synthetic route to lead magnesium niobate and lead iron niobate. *J. Eur. Ceram. Soc.*, 1998, **19**, 155–163.
10. Ananta, S., and Thomas, N. W., Relationships between sintering conditions, microstructure and dielectric properties of lead magnesium niobate. *J. Europ. Ceram. Soc.*, submitted for publication.
11. Ananta, S., Brydson, R. and Thomas, N. W., Synthesis, formation and characterisation of $FeNbO_4$ powders. *J. Eur. Ceram. Soc.*, submitted for publication.
12. Schmidbauer, E. and Schneider, J., Electrical resistivity, thermopower, and ^{57}Fe Mossbauer study of $FeNbO_4$. *J. Solid State Chem.*, 1997, **134**, 253–264.
13. Chiu, C. C. and Desu, S. B., Microstructure and properties of lead ferroelectric ceramics ($Pb(Fe_{0\cdot5}Nb_{0\cdot5})O_3$). *Mater. Sci. Eng.*, 1993, **B21**, 26–35.